Trapping of Single-Cells Within 3D Electrokinetic Cages

Kevin Keim[1], António Gonçalves[1], Carlotta Guiducci[1]

1. École Polytechnique Fédérale de Lausanne - Laboratory of Life Sciences Electronics (Guiducci Lab), Station 17 CH-1015 Lausanne, Switzerland

Introduction

Single-cell analysis (SCA) refers to the analysis of single cells in a sample instead of average measurements of the cells ensemble. Bulk experiments might lead to misleading interpretations, while observing a single cell gives indications about the specific cell phenotype [1]. Cell populations, especially of diseased cells, are heterogeneous. SCA of cell populations can finely describe their heterogeneity and identify minorities [2].

In order to observe a single cell, the clone has to be taken from the bulk and isolated. SCA becomes especially meaningful, if many single-cells can be observed concomitantly over time [3]. Therefore, methods were developed to array single-cells in order to investigate them in a simultaneous manner. Microwells, patterns or single-cell traps are examples to immobilize cells at fixed locations on a surface [4]. Negative dielectrophoretic (nDEP) traps can capture cells at electric field minima in suspension [5], [6].
For nDEP traps, three-dimensional electrodes are advantageous, since they create homogeneous electric fields and therefore create an equal trapping force over the complete height of a microfluidic channel, when placed within. Our group has recently developed a fabrication process, with which we can fabricate three-dimensional electrodes of any shape and high aspect ratio [7], a SEM micrograph of these electrodes is shown in Fig. 1. These electrodes have already been used for in flow impedance measurements, electrorotation and deterministic lateral displacement devices with implemented DEP fine tuning [8]–[10]. Now, we want to use these electrodes for nDEP trapping devices. We fabricated two arrays of three-dimensional electrodes and apply AC electric fields of different amplitudes between the first row of electrodes and the second row. These creates two dielectric barriers, a first, lower entry barrier and a second higher exit barrier. Cells are supposed to overcome the first barrier and get trapped at the second barrier, so we can perform analysis on these arrayed and separated single cells. In order to find the correct trap dimensions and experimental conditions, we perform finite elements simulations, using COMSOL Multiphysics®.

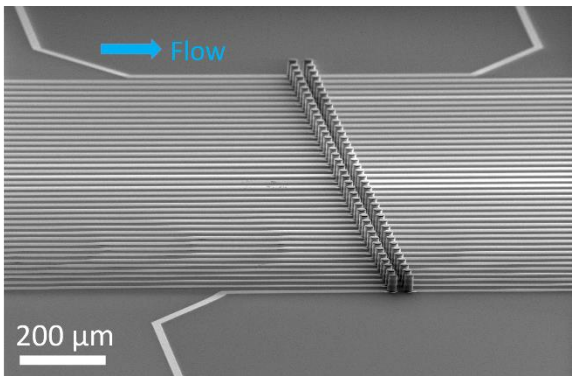

Figure 1. SEM micrograph of an array of 3D electrodes.

Theory

Dielectrophoresis is a phenomenon, in which polarizable particles experience a force in inhomogeneous electric field. The electric field polarizes the particles and the charges within the particles are dislocated. Due to the inhomogeneity, the electric field at one side of the particle is higher than at the other side. Consequently, one electrostatic force is stronger than the other and a net force is exerted on the particle. The dielectrophoretic force is given by [11]

$$\langle \mathbf{F}_{\mathrm{DEP}} \rangle = \pi \varepsilon_0 \varepsilon_m \mathrm{R}^3 Re[\mathrm{CM}] \nabla E_{pk}^2 \quad (1)$$

ε_0 is the absolute and ε_m is the relative permittivity of the medium; R is the cell radius and *Re*[CM] is the real part of the Clausius-Mossotti (CM) factor, which depends on the dielectric properties of the cell and the surrounding medium. ∇E_{pk}^2 is the gradient of the peak electric field.

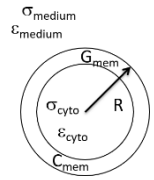

Figure 2. Illustration of the single-shell model used in the simulations.

In an AC electric field, the effects of the net charge of the particle cancels out and only the polarizability of the particle matters. However, the polarizability depends on the particle and the surrounding medium and is reflected in the CM factor. If the particle is more polarizable then the surrounding medium, it will move towards high field regions and one talks of positive DEP (pDEP). If it is less polarizable than the surrounding medium, it will move toward lower field region, called nDEP. This is reflected in the real part of

the CM factor for the single shell model, illustrated in Fig. 2, given by

$$\mathrm{CM} = \frac{\tilde{\varepsilon}_p - \tilde{\varepsilon}_m}{\tilde{\varepsilon}_p + 2\tilde{\varepsilon}_m}; \quad \tilde{\varepsilon}_p = \tilde{C}_{mem} \frac{3R\tilde{\varepsilon}_{cyto}}{3\tilde{\varepsilon}_{cyto} + 3\tilde{C}_{mem}R} \qquad (2)$$

$\tilde{\varepsilon}_p$, $\tilde{\varepsilon}_m$, $\tilde{\varepsilon}_{cyto}$ are the complex permittivity of the particle, the suspending medium and the cytoplasm, defined as: $\tilde{\varepsilon} = \varepsilon - \frac{i\sigma}{\omega}$ and $\tilde{C}_{mem}$ is the complex membrane capacitance defined as $\tilde{C} = C - \frac{iG}{\omega}$ with G the membrane conductance [12].

Besides the DEP force, another force is acting on the cells simultaneously, while in the microfluidic channel.

$$\langle \boldsymbol{F}_{drag} \rangle = -6\pi\eta R\boldsymbol{v} \qquad (3)$$

Is the microfluidic drag force, which depends on the medium viscosity η, the particle radius R and the velocity of the fluid $\boldsymbol{v}$. A cell can be trapped in suspension if there is no net force acting on it, so if Eq. 1 and Eq. 2 are equal and there is no initial velocity of the cell. A possibility to create this is by applying a specific voltage at the electrode arrays, which create dielectric barriers and exert a force, which compensates the drag force, as shown in Fig. 3.

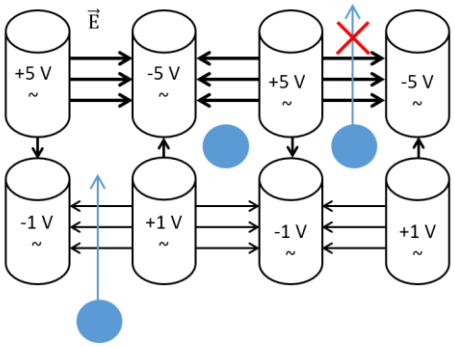

Figure 3. Cells trapped in an electrodes array with two different dielectric barriers. The cell (left) overcomes the first dielectric barrier due to the microfluidic drag force, but cannot overcome the second barrier (right) and is trapped in the array.

Methods

Finite elements simulations forecast the trajectory of cells in certain electrode geometries and experimental conditions. We create a cuboid of 400 µm per 400 µm per 50 µm of the electrode configuration, by creating a working plane of 400 µm per 400 µm and implementing the ground plane of the electrode (diameter and inter electrode distance of 20 µm, 40 µm and 80 µm) configuration. Subsequently we extrude this plane by 50 µm. Next, we introduce the electric current and laminar flow physics. The properties of water are given to the active volume of the device. We create a fluid inlet at one side, by applying a pressure between 0.01 mbar and 1 mbar and creating an outlet of 0 mbar at the opposite side.

We assign an alternating electric potential of -1V and +1V to the upstream and of -5V and +5V at the downstream electrodes. In a first stationary study we solve the laminar flow and electric current equations. The results are illustrated in the plot of the pressure and fluid streamlines, shown in Fig. 3, and in the plot of the absolute value of the electric field and the electric field lines, shown in Fig. 4.

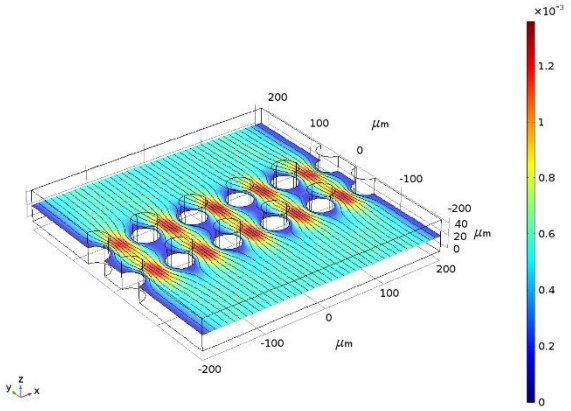

Figure 4. Illustration of the simulated pressure and the fluid flow streamlines in the 3D electrode array.

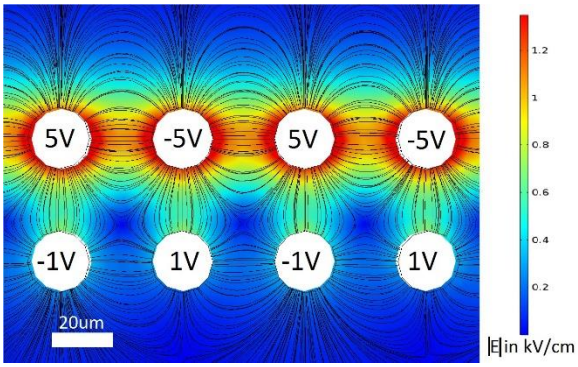

Figure 5. Illustration of the absolute value of the electric field and the electric field lines.

Using the results of the first stationary study, we compute a time dependent study, analyzing the cells trajectory, with the particle tracing for fluid flow module. We create a particle inlet at the same boundary as the fluid inlet and a particle outlet at the fluid outlet. At t = 0 s we release twenty solid particles at a density based position in the channel with the initial velocity based on based on the velocity field, previously calculated. The forces acting on the particles are set to be the fluid drag force, as given in

Eq. 2, which is already implemented in COMSOL® and the dielectric force, given by Eq.1, which we implemented ourselves in order to be able to use the CM factor, based on the complex membrane capacitance, shown in Eq. 3.

We performed this study sweeping the conductivity of the surrounding medium between 1m S/m and 1000 mS/m, as well as the electric field frequencies between 100 kHz and 10 MHz for human T lymphocytes, A549, M17 neuroblastoma, HEK 293 and HeLa cells. The dielectric parameters used for these cells are given in Table 1. After the simulations the trajectory and the final position of the cells are illustrated in the three-dimensional space and a statement about the functionality of the trapping in the given conditions can be made.

	C_{mem}	G_{mem}	R	σ_{cyto}	ε_{cyto}	Ref
T lymphocytes	7.01 mF/m^2	1345 S/m^2	3.6 µm	0.53 S/m	100	[13]
A549	16.95 mF/m^2	1345 S/m^2	3.45 µm	0.23 S/m	100	[13]
M17	16.95 mF/m^2	800 S/m^2	6.9 µm	0.23 S/m	100	[14]
HEK 293	7.94 mF/m^2	0	6.5 µm	0.408 S/m	85	[15]
HeLa	19.9 mF/m^2	0	10.5 µm	0.32 S/m	85	[16], [17]

Table 1: Dielectric parameters of the cells used in the simulations.

Results and Discussion

We performed this finite element study in order to find the experimental parameters and geometries to trap cells in the electrode array in order to perform subsequently electrorotation experiments with them. In what follows we present the parameters we tuned to achieve efficient DEP trapping.

1. Effect of the medium conductivity and the electric field frequency on the trapping efficiency

In order to find the correct trapping conditions, first the dielectrophoretic force has to be negative, since we want to trap the cells in suspension within the electrode array. To find the DEP force, given in Eq. 1, negative, the CM factor, given in Eq. 3, has to be negative. To ensure the correct values of this factor within COMSOL®, we plot this factor for the different cell values given in Table 1. The CM factor, depending on the frequency of the AC electric field for each cell at a medium conductivity of 100 mS/m, is shown in Fig. 6. The CM factor is plotted in COMSOL Multiphysics©, and ensures therefore the correct value for the simulations.

Different cells experience different DEP forces, depending on their CM factors. In the experiments, we used a medium conductivity of 100 mS/m, since the imaginary part of the CM factor needs to be negative, in order to have trapping, but the real part has to be distinct in order to extract the cells dielectric parameters by electrorotation [18].

The CM factor depends strongly on the medium conductivity, as shown in Fig. 7. In order to achieve nDEP for T lymphocytes, the medium conductivity cannot be set below 10 mS/m. Even with this medium conductivity the CM factor is never below -0.2, which directly results in a reduced DEP trapping force, given in Eq. 1. The higher the medium conductivity the stronger the DEP trapping force. At 100 mS/m medium conductivity, the CM factor below 100 kHz is not at its minimum of -0.5, but close with a value below -0.45.

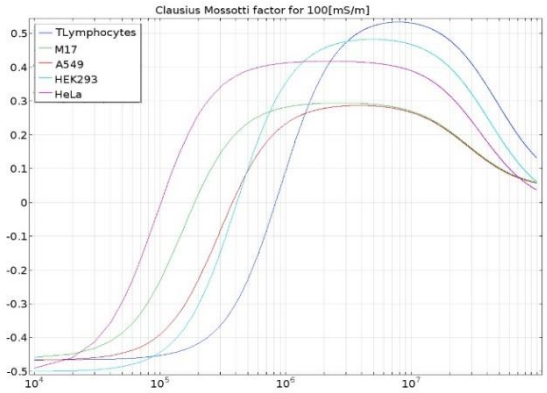

Figure 6. Clausius-Mossotti factor of different cells depending on the frequency of the electric field for medium conductivity of 100 mS/m.

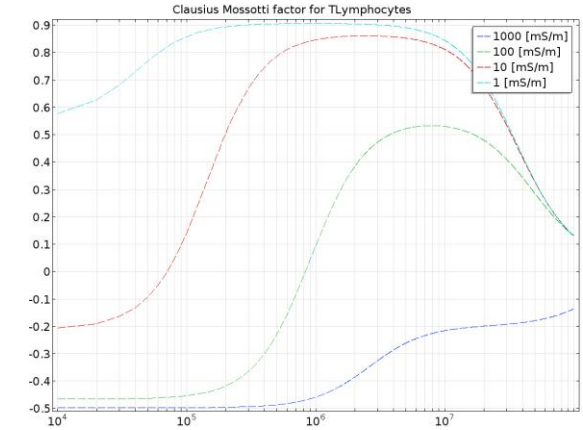

Figure 7. Clausius-Mossotti factor of T lymphocytes depending on the medium conductivity.

If the experimental conditions are not adapted and the DEP force is positive, the cells will not be trapped in the middle of the electrode array in open space, but will go towards high field regions and thus towards the electrodes' surface, as shown in Fig. 8.

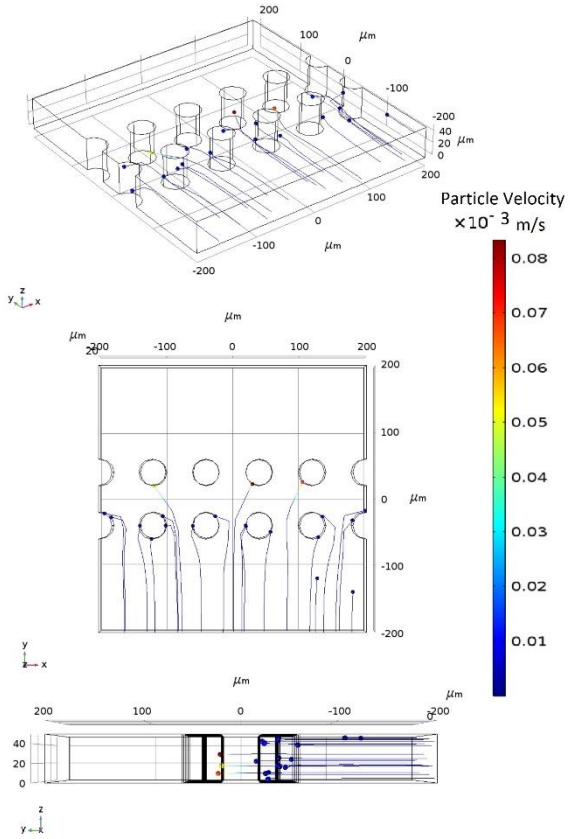

Figure 8. Perspective view (top), top view (middle) and side view (bottom) of T lymphocytes getting trapped on the electrodes due to the pDEP force. The medium conductivity is 100 mS/m and the frequency of the electric field is 10 MHz.

Applying the correct experimental conditions, for example, 100 kHz and 1000 mS/m for T lymphocytes, the cells are getting trapped in between the electrodes as shown in Fig. 9.

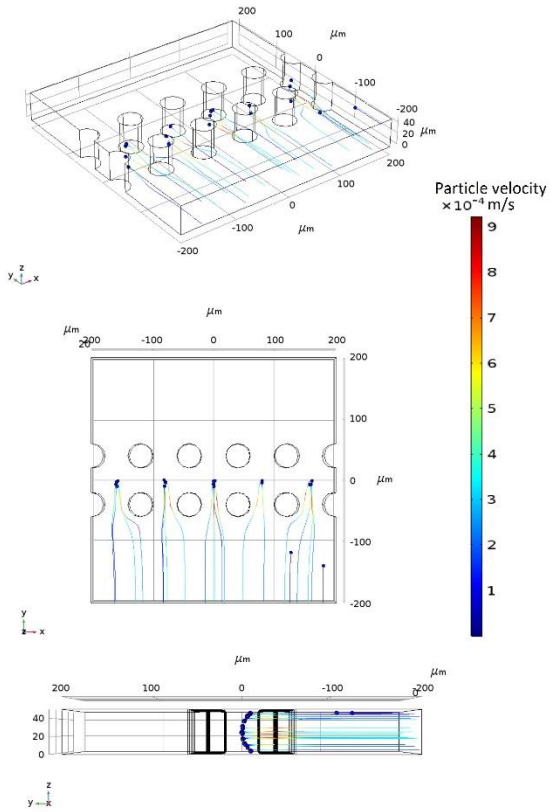

Figure 9. Perspective view (top), top view (middle) and side view (bottom) of T lymphocytes getting trapped in between the electrodes due to the nDEP force. The medium conductivity is 1000 mS/m and the frequency of the electric field is 100 kHz.

The experimental conditions of medium conductivity and electric field frequency have to be adapted. A first indication is the CM factor. Additionally finite elements simulations help illustrating and, finally, the experimental investigation has to be done.

2. Effect of the microfluidic pressure

Once the medium conductivity and the electric field frequency are found, the pressure of the fluid flow has to be adapted. The DEP trapping force, given in Eq. 1, and the fluid drag force, given in Eq. 2 have to cancel out inside the micro cage array and the initial velocity of the cell at the time it come to this point has to be neutral. Tuning the DEP force for the trapping in the first results section, we are now tuning the pressure and therefore the drag force in order to achieve trapping inside the array.

Working in nDEP conditions with a fixed electrode size, three scenarios for different pressures are possible. First, the pressure and therefore the drag

force is not sufficient to overcome the first, lower dielectric entrance barrier. The cells are stopped by the dielectrophoretic force before entering the micro cage array as shown in Fig. 10.

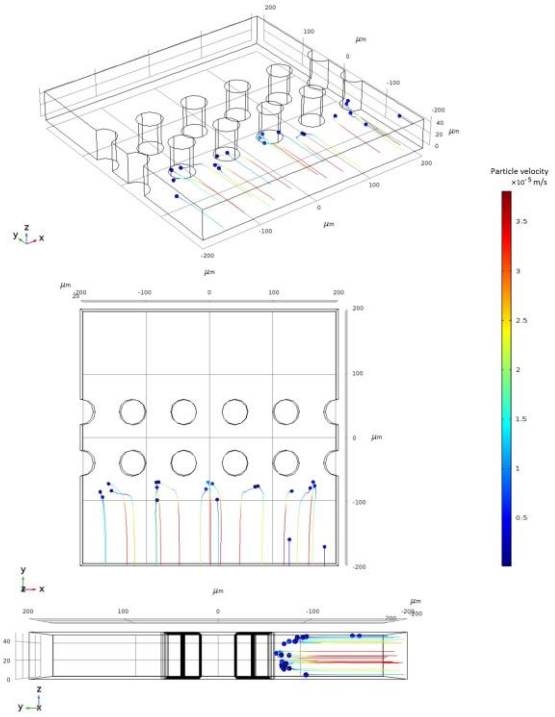

Figure 10. Perspective (top) and top (bottom) view of T lymphocytes prevented to access the micro cage space for a pressure difference of 0.01 mbar between inlet and outlet.

Second, if the pressure difference between the inlet and outlet, the drag force is always stronger then the DEP trapping force. The cells slow down inside the DEP trap, as seen in the velocity of the cells illustrated in the color of the trajectory in Fig. 11. However, in the end the cells get across the highest electric field between the downstream (exit) electrodes and are even accelerated by the DEP force, when they have passed the exit electrodes.

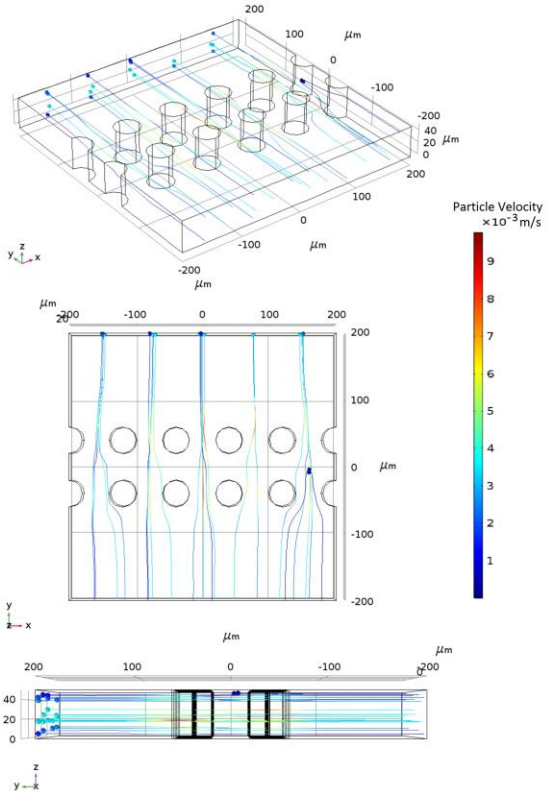

Figure 11. Perspective (top) and top (bottom) view of T lymphocytes flowing through the micro cage array for a pressure difference of 1 mbar between inlet and outlet. The cells decelerate in the trap, but reaccelerate when they leave the trap.

Adapting the pressure to the correct value allows trapping the cells within the micro cage array. The cells have to pass the first dielectric barrier. While approaching the local maximal value of the electric field in between the entrance electrodes, the cell slows down, but once it passes it, it reaccelerates. The restriction of the flow, between the electrodes, increases the speed of the cell additionally. However, this restriction is not present inside the trap. The second strong barrier eventually stops the cell completely and pushes it towards the local energy minimum, out of fluidic flow potential energy and dielectrophoretic potential energy. In this energy minimum, the force, which is the derivation of the energy in space, is zero. The trapping of the cells is illustrated in Fig. 12.

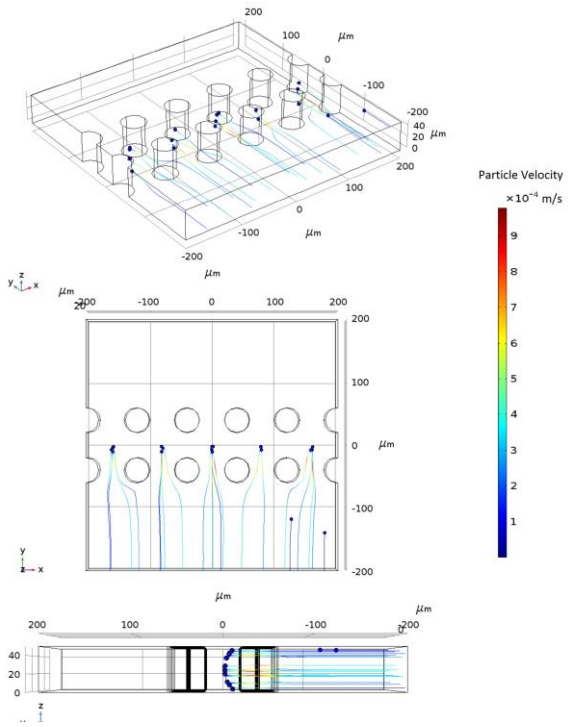

Figure 12. Perspective (top) and top (bottom) view of T lymphocytes trapped in the micro cage array for a pressure difference of 0.1 mbar between inlet and outlet. The cells accelerate, when passing the first dielectric barrier, but get eventually trapped.

3. Impact of the trap size

The last external parameter we are tuning is the trap size, which is defined as the distance between the electrode distance and which is at the same time the electrodes diameter. First, reducing trap size obviously increases the electric field, since the same voltage is applied over a shorter distance. Second, it changes the curvature of the electric field too. Since the DEP force, given in Eq. 1, depends on the gradient of the electric field squared $\nabla \boldsymbol{E}_{\boldsymbol{pk}}^{\boldsymbol{2}}$, as illustrated in Fig. 13, it changes with the trap size.

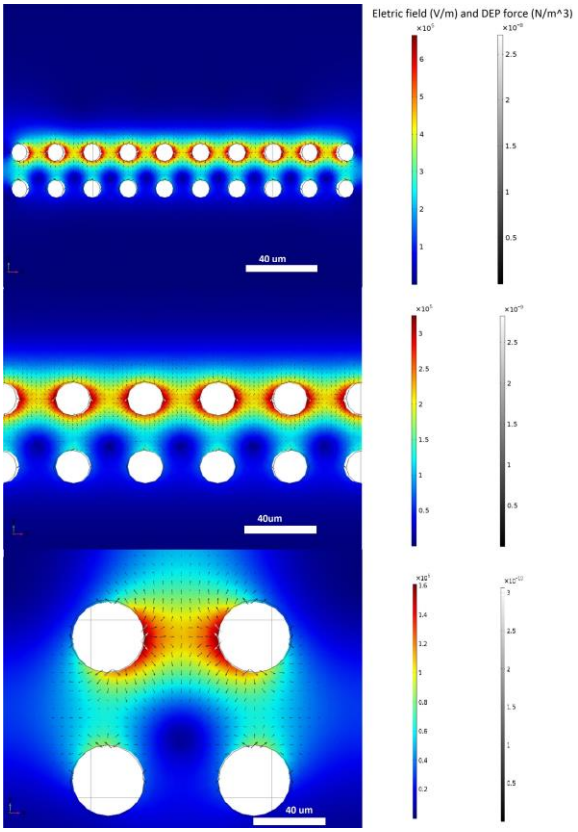

Figure 13. Illustration of the absolute value of the electric field and the corresponding DEP force. The DEP force increase, when decreasing the electrode distance (top: 80 µm; middle: 40 µm; bottom: 20 µm), due to the increase electric field and the increased gradient of the field.

This variation of the trapping force, is as well reflected in the trapping behavior of the cells. A549 cells for example with a pressure of 0.1 mbar are not entering the electrode array, if the inter electrode distance is 20 µm, they are getting trapped in the array, if the inter electrode distance is 40 µm and are flowing through the electrode array if the inter electrode distance is 80 µm, as shown in Fig. 14.

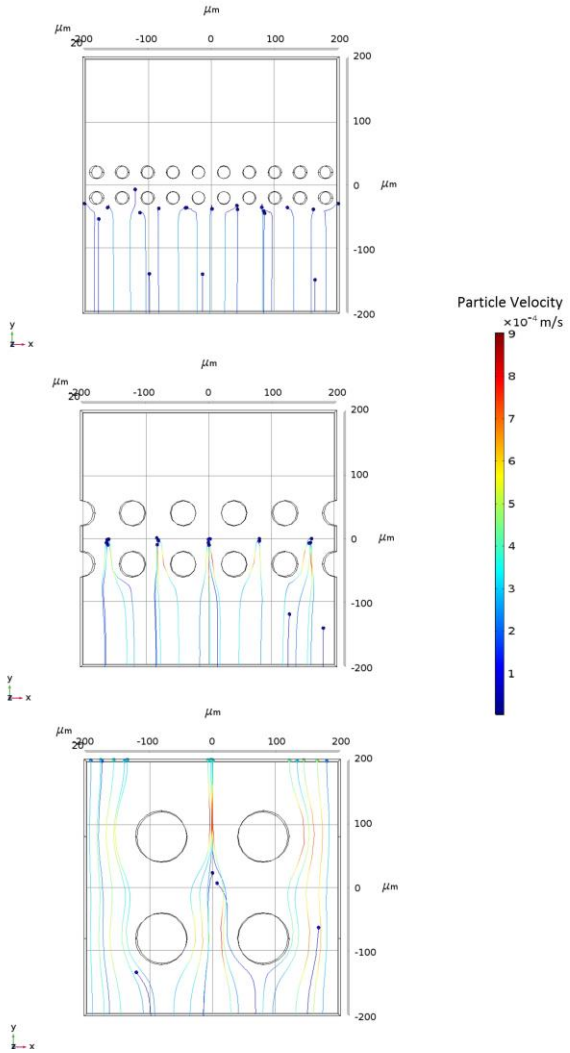

Figure 14. A549 cells for a pressure of 0.1 mbar are not entering the electrode array for a inter electrode distance of 20 µm are not entering the electrode array (top). For an inter electrode distance of 40 µm, they are getting trapped (middle) and for an inter electrode distance of 80 µm (bottom) they are flowing through the array.

4. Trapping efficiency for different cell types

As already partially discussed in the first results section, the CM factor depends on the cells dielectric properties. Different cells have different CM factor and radii, consequently they have different trapping behaviors. It turns out, that for the exact same conditions, some cell types are getting trapped and others are not, as shown in Fig. 15 for M17 cells and T lymphocytes and in Fig. 16 for HeLa and HEK 293 cells.

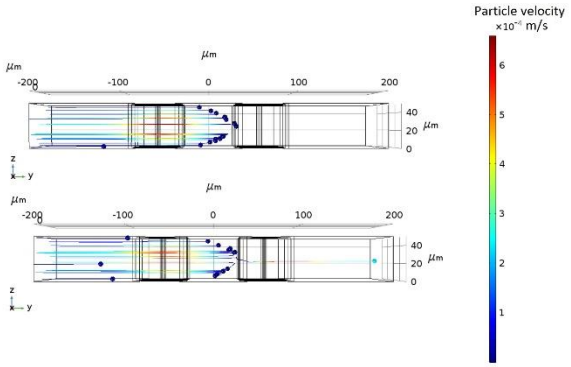

Figure 15. At a pressure of 0.07 mbar and an inter electrode distance of 40 µm and an electric field frequency of 2 MHz, M17 cells (top) are all getting trapped, while some T lymphocytes (bottom) are flowing through the array.

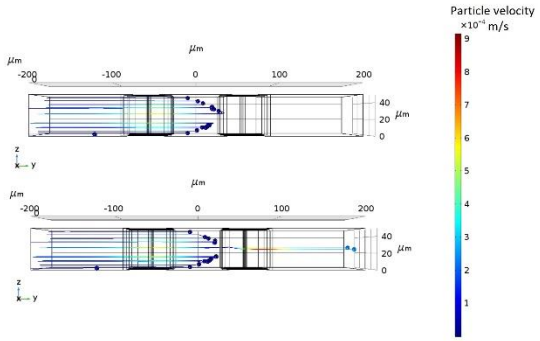

Figure 16. At a pressure of 0.06 mbar and an inter electrode distance of 40 µm and an electric field frequency of 2.3 MHz, HeLa cells (top) are all getting trapped, while some HEK 293 (bottom) are flowing through the array.

The different tapping behavior of different cells leads to the conclusion, that there is not one uniform experimental condition for all cell types, but specific ones for specific cell types. Therefore, in order to predict trapping of a certain cell type, finite element simulations with the specific dielectric parameters of the cells have to be performed.

Conclusions

In this paper, we present finite elements simulations, using COMSOL Multiphysics®, in which predict the trapping behavior of our nDEP traps. We could find trapping conditions for each of the cells, we considered. We investigated the effects of the frequency of the electric field, the medium conductivity as well as the trap size. Due to the diversity of cells we used, we did not find one configuration, which suits all needs, but we can simulate the behavior for every specific case.

References

[1] D. Di Carlo and L. P. Lee, "Dynamic Single-Cell Analysis for Quantitative Biology," *Anal. Chem.*, vol. 78, no. 23, pp. 7918–7925, Dec. 2006.

[2] H. A. Svahn and A. van den Berg, "Single cells or large populations?," *Lab Chip*, vol. 7, no. 5, pp. 544–546, 2007.

[3] G. R. Sant, K. B. Knopf, and D. M. Albala, "Live-single-cell phenotypic cancer biomarkers-future role in precision oncology?," *npj Precis. Oncol.*, vol. 1, no. 1, p. 21, 2017.

[4] S. Lindström and H. Andersson-Svahn, "Overview of single-cell analyses: microdevices and applications," *Lab Chip*, vol. 10, no. 207890, pp. 3663–3672, 2010.

[5] J. Voldman, M. L. Gray, M. Toner, and M. A. Schmidt, "A Microfabrication-Based Dynamic Array Cytometer," *Anal. Chem.*, vol. 74, no. 16, pp. 3984–3990, Aug. 2002.

[6] N. Manaresi *et al.*, "A cmos chip for individual cell manipulation and detection," *IEEE J. Solid-State Circuits*, vol. 38, no. 12, pp. 2297–2305, Dec. 2003.

[7] S. C. Kilchenmann, E. Rollo, P. Maoddi, and C. Guiducci, "Metal-Coated SU-8 Structures for High-Density 3-D Microelectrode Arrays," *Journal of Microelectromechanical Systems*, vol. 25, no. 3, pp. 425–431, Jun-2016.

[8] K. Keim, P. Maoddi, S. Kilchenmann, M. Comino, and C. Guiduccci, "Lab-on-a-Chip Platform for Single-Cell Electrorotation Using 3D Electrodes," in *microTAS*, 2017, pp. 932–934.

[9] E. Rollo *et al.*, "Label-free identification of activated T lymphocytes through tridimensional microsensors on chip," *Biosensors*, 2017.

[10] J. P. Beech, K. Keim, B. D. Ho, O. Ström, and J. O. Tegenfeldt, "Tuable separation and DNA manipulation in metal coated pillar arrays," in *microTAS*, 2018.

[11] R. Pethig, *Dielectrophoresis*. Chichester, UK: John Wiley & Sons, Ltd, 2017.

[12] P. R. C. Gascoyne, F. F. Becker, and X. B. Wang, "Numerical analysis of the influence of experimental conditions on the accuracy of dielectric parameters derived from electrorotation measurements," *Bioelectrochemistry Bioenerg.*, vol. 36, no. 2, pp. 115–125, 1995.

[13] S.-I. Han, Y.-D. Joo, and K.-H. Han, "An electrorotation technique for measuring the dielectric properties of cells with simultaneous use of negative quadrupolar dielectrophoresis and electrorotation.," *Analyst*, vol. 138, no. 5, pp. 1529–37, 2013.

[14] S. Kilchenmann, P. G. Carlotta, P. P. Demetri, and P. H. M. P, "Microfluidic and Electrokinetic Manipulation of Single Cells," 2016.

[15] A. El-Gaddar, M. Frénéa-Robin, D. Voyer, H. Aka, N. Haddour, and L. Krähenbühl, "Assessment of 0.5 T Static Field Exposure Effect on Yeast and HEK Cells Using Electrorotation," *Biophys. J.*, vol. 104, no. 8, pp. 1805–1811, Apr. 2013.

[16] R. T. K. Kumar, K. Cherukuri, R. Chadha, V. Holderby, and S. Prasad, "Planar biochip system for combinatorial electrokinetics," *Biochip J.*, vol. 10, no. 2, pp. 131–139, 2016.

[17] F. Y. Chang, M. K. Chen, M. H. Wang, and L. S. Jang, "Electrical Properties of HeLa Cells Based on Scalable 3D Interdigital Electrode Array," *Electroanalysis*, vol. 28, no. 5, pp. 962–969, 2016.

[18] K. Keim, P. Éry, A. Delattre, and C. Guiducci, "3D electrode arrays for trapping, analysis and selectrive release of single cells using DEP," in *Micro Total Analysis Systems*, 2018.

Acknowledgements

We would like to thank COMSOL® Switzerland and especially Thierry Luthy for support, setting up the simulations. Many thanks to the Scientific IT and Application support of EPFL, which provided us guidance and support in using the EPFL cluster to compute some of the simulations. This work was finance by the Swiss National Science Foundation (205321_179086).

Contact

kevin.keim@epfl.ch; +41 21 69 31335